

Compressibility and wall-cooling effects on high-speed turbulent boundary layers

Michele Cogo^{1*}, Mauro Chinappi², Matteo Bernardini³, and Francesco Picano^{1,4}

¹ Centro di Ateneo di Studi e Attività Spaziali 'Giuseppe Colombo' (CISAS), Università degli Studi di Padova, via Venezia 15, 35131 Padua, Italy

² Department of Industrial Engineering, University of Rome Tor Vergata, via del Politecnico 1, 00133 Rome, Italy

³ Department of Mechanical and Aerospace Engineering, Sapienza University of Rome, via Eudossiana 18, 00184 Rome, Italy

⁴ Department of Industrial Engineering, Università degli Studi di Padova, via Venezia 1, 35131 Padua, Italy

*michele.cogo.1@phd.unipd.it

Keywords: Compressible Boundary Layers, Turbulent Boundary Layers

Abstract. Flight systems operating at high speeds are frequently enveloped by turbulent, hot, highly compressible flow experiencing various regimes in terms of Mach numbers and surface temperature. These factors are dominant in the proximity of the surface, the boundary layer, posing technical difficulties in predicting the mechanical and thermal loads. In this work, we analyze a database of Direct numerical Simulations of turbulent boundary layers for Mach numbers 2, 4 and 6 and four different wall temperatures (from adiabatic to cold wall). We discuss the choice of the diabatic parameter to define the degree of wall-cooling across different Mach numbers, observing its influence on instantaneous fields and first-second order velocity and temperature statistics.

Introduction and database setup

High speed turbulent boundary layers represent a fundamental case study to determine the aerodynamic heating and drag acting on supersonic and hypersonic vehicles.

As the velocity of the freestream flow becomes several times larger than the speed of sound, i.e. the Mach number increases, compressibility influences the mean and fluctuating fields of thermodynamic quantities, which are coupled to the momentum through density. When this high-speed flow is brought to rest by the friction with the wall, it is important to consider the amount of kinetic energy that can be converted to thermal, which can be quantified looking at the recovery temperature $T_r = T_\infty(1 + r(\gamma - 1)/2M_\infty^2)$ with $r = Pr^{1/3}$ the recovery factor, since the process is non-isentropic.

In the case that the wall only exchanges heat with the flow for long times, reaching the recovery temperature, the temperature profile would reach a zero-gradient slope, settling in an adiabatic condition.

However, in practical cases, the vehicle surface is usually expected to be at lower temperatures, i.e. $T_w/T_r < 1$, generating large heat fluxes to the wall (cold wall). This affects the flow dynamics in conjunction with the Mach number, enriching the physical effects that need consideration in the formulation of theoretical relations and models.

The presence of a cold wall leads to an alteration in the mean temperature gradient's sign near the wall. This change influences the generation of temperature fluctuations, potentially causing a significant deviation from the similarity between velocity and temperature fields, a building block of theory of compressible flows [6]. This loss of similarity is evident in instantaneous snapshots of turbulent structures [3]. However, this study also noted that the same T_w/T_r condition at

different Mach numbers resulted in very different near-wall dynamics for temperature fluctuations, being more similar to velocity at high Mach numbers. Recently, other definitions of the wall temperature condition have been proposed, such as the diabatic parameter $\Theta = (T_w - T_\infty)/(T_r - T_\infty)$ which are capable to account for the indirect effect of Mach number on the wall temperature condition. In fact, this parameter only takes in to account the ΔT that is recovered when the flow is brought at rest, being the only one responsible for kinetic-internal energy exchanges.

In this work, we aim to leverage the diabatic parameter Θ to analyse the interplay of the Mach number and wall temperature condition, discussing their respective imprints on turbulence statistics.

To pursue this objective, an extensive Direct Numerical Simulation (DNS) database consisting of 12 simulations of zero-pressure-gradient turbulent boundary layers has been computed fixing the friction Reynolds number, while spanning three Mach numbers $M_\infty = [2, 4, 6]$ and four diabatic parameters $\Theta = \{0.25, 0.5, 0.75, 1.0\}$, going from extremely cold walls, $\Theta = 0.25$, to adiabatic case, $\Theta = 1$.

Information concerning the domain size, grid resolution and boundary layer properties at selected stations (where $Re_\tau = 443$) are available at reference [4].

Here, M_∞ is the free-stream Mach number and Re_τ is the friction Reynolds number, defined as the ratio between the boundary layer thickness δ_{99} and the viscous length scale $\delta_v = \nu_w/u_\tau$, where $u_\tau = \sqrt{\tau_w/\rho_w}$ is the friction velocity, τ_w is the mean wall shear stress, and ν_w is the kinematic viscosity at the wall. Moreover, $y^* = y/\delta_{v,SL}$ is the semilocal scaled wall-normal coordinate, with $\delta_{v,SL} = \nu/\sqrt{\tau_w/\rho}$.

The Navier–Stokes equations are solved using STREAMS [2], an open-source numerical solver for compressible flows oriented to modern HPC platforms using MPI parallelization and supporting multi-GPU architectures under the CUDA paradigm. In shock-free regions, the convective terms are evaluated using high-order energy preserving schemes, while a shock capturing formulation is activated with a Ducros sensor. The diffusive terms are discretized using a locally conservative scheme expanded to standard Laplacian formulation.

Results

We first consider the instantaneous field in the form of wall-parallel slices of velocity and temperature fluctuations, Figure 1. The slices are selected at a wall-normal location $y^* = 10$, which is approximately coincident with the peak of streamwise velocity fluctuations in the buffer layer [4]. Here, we selected the two extreme cases of the diabatic parameter $\Theta = \{0.25, 1\}$ and Mach numbers $M_\infty = \{2, 6\}$.

As expected, all cases show the presence of near-wall streaks for velocity fluctuations with similar intensities, a sign of the near-wall self-sustaining cycle of turbulence.

However, the picture is clearly different for temperature fluctuations. While adiabatic cases maintain a streaky pattern very similar to the velocity counterpart, showing a clear temperature-velocity coupling, cold cases ($\Theta = 0.25$) show highly damped fluctuations with an absence of elongated streaks.

These qualitative results preliminarily show two aspects: the first is that cold walls reduce the temperature-velocity coupling in the buffer layer, highly damping temperature fluctuations. The second aspect is that fixing the diabatic parameter yields the same general behavior due to the effect of wall-cooling at different Mach numbers.

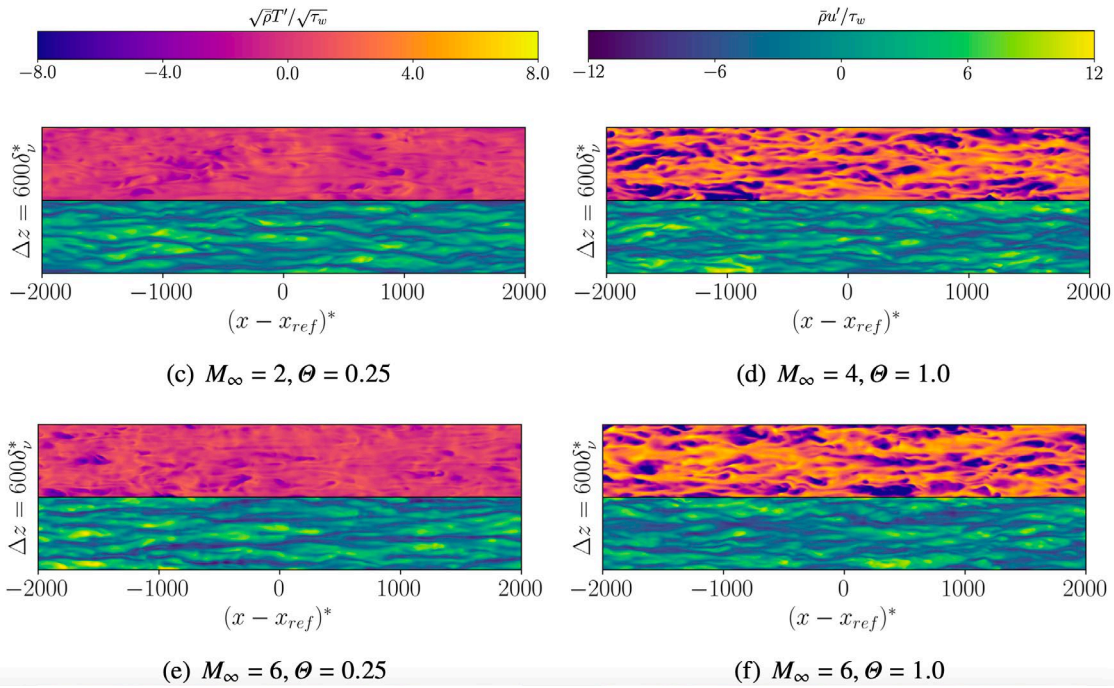


Figure 1: Temperature (top) and streamwise velocity (bottom) fluctuations in wall-parallel slices (x - z plane) selected at $y^* \approx 10$. Here, only the cases at Mach numbers 2 and 4 are shown with the respective extremes in $\theta = \{0.25, 1\}$.

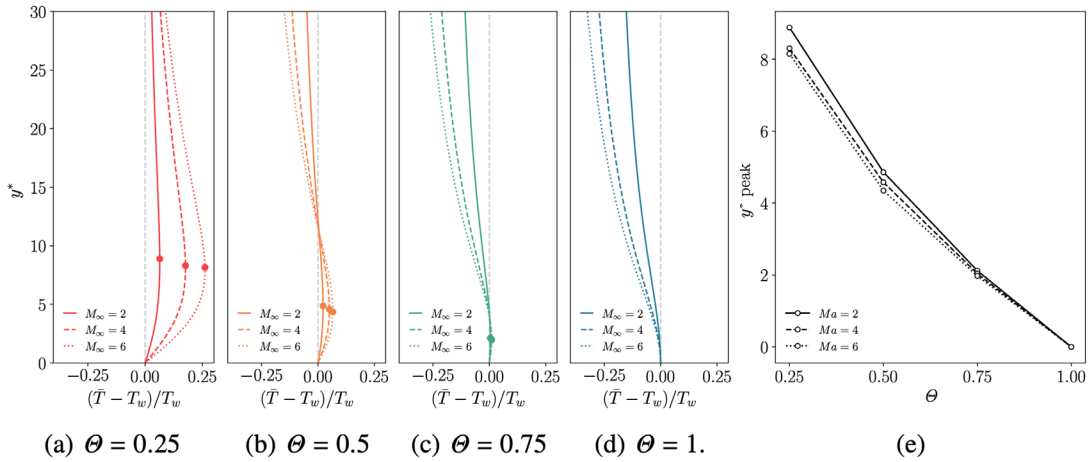


Figure 2: Panels (a-b-c-d): Mean temperature profiles scaled with T_w and relative peaks as function of the wall-normal coordinate y^* . Panel (e): Wall-normal location of mean temperature peaks as function of the diabatic parameter θ .

An insight on the underlying physics regulating the decoupling between temperature and velocity fluctuations can be obtained by looking at wall-normal mean temperature profiles, Figure 2. As the Mach number increases, the recovery temperature at which the flow would like to settle at the wall increases (quadratically with M_∞). However, a cold wall condition ($T_w < T_r$) forces the temperature profile to slant towards colder temperature, resulting in a local peak, evident in Figure 2(a). Here, it is also evident that the prominence of this peak is depended on the Mach number, and gives rise to the aerodynamic heating, generating a net heat flux from the flow to the solid boundary. Local temperature peaks are marked in figures 2(a) to 2(d) with dots for all diabatic parameters. An increase in the Mach number generates more intense gradients and higher peak temperatures for non-adiabatic cases, enhancing aerodynamic heating. However, the wall-normal

location of the peaks is mainly dependent by the change θ , and only weakly dependent on the Mach number. This is visible in Figure 2(e), which shows a departure from the wall of the peak location as θ decreases. Given that the mean temperature gradient is directly connected to thermal production, $P_T = -\bar{\rho} \overline{v''T''} \partial\bar{T}/\partial y$ (refer to [5]), and that for the cases ($\theta = 0.25$) $\partial\bar{T}/\partial y \approx 0$ at $y^* \approx 10$, when can see why temperature fluctuations are highly damped in this region. As a result, we observe an absence of near-wall streaks and a reduction of their overall intensity, as visible in Figure 1.

Conclusions

In this study, we presented a database of 12 DNS highlighting the effect of the Mach number and wall-cooling on zero-pressure-gradient turbulent boundary layers.

The instantaneous flow organization revealed strong differences from temperature and velocity fields as the wall-cooling increased, which were visible at all Mach numbers when fixing the diabatic parameter θ , a sign of its aptness to yield the same wall-cooling effects across different M_∞ .

The temperature-velocity decoupling for cold cases can be explained by looking at the mean temperature profiles, knowing their influence in the thermal production term. We observed that as the wall-cooling increases, there is a formation of a local mean temperature peak that rises in the wall-normal direction. In our coldest case ($\theta = 0.25$), the location of the peak approaches the buffer layer, highly damping the temperature fluctuations and their correlations with velocity.

References

- [1] Zhang, Y. S., Bi, W. T., Hussain, F., & She, Z. S. (2014). A generalized Reynolds analogy for compressible wall-bounded turbulent flows. *Journal of Fluid Mechanics*, 739, 392-420. <https://doi.org/10.1017/jfm.2013.620>
- [2] M. Bernardini, D. Modesti, F. Salvatore, S. Sathyanarayana, G. Della Posta, and S. Pirozzoli. Streams-2.0: Supersonic turbulent accelerated navier-stokes solver version 2.0. *Comput. Phys. Commun.*, 285:108644, 2023. <https://doi.org/10.1016/j.cpc.2022.108644>
- [3] Cogo, M., Salvatore, F., Picano, F., & Bernardini, M. (2022). Direct numerical simulation of supersonic and hypersonic turbulent boundary layers at moderate-high Reynolds numbers and isothermal wall condition. *Journal of Fluid Mechanics*, 945, A30. <https://doi.org/10.1017/jfm.2022.574>
- [4] Cogo M, Baù U, Chinappi M, Bernardini M, Picano F. Assessment of heat transfer and Mach number effects on high-speed turbulent boundary layers. *Journal of Fluid Mechanics*. 2023;974:A10. <https://doi.org/10.1017/jfm.2023.791>
- [5] T. B. Gatski and J. P. Bonnet. *Compressibility, turbulence and high speed flow*. Academic Press, 2013.
- [6] Morkovin, M.V. 1962 Effects of compressibility on turbulent flows. *Méc. Turbul.* 367(380),26